

## 1-(2-Pyridylazo)-2-naphthol modified carbon paste electrode for trace cobalt(II) determination by differential pulse cathodic voltammetry

Miriam Rehana Khan and Soo Beng Khoo\*

Department of Chemistry, National University of Singapore, Singapore 119260, Singapore

**A differential pulse cathodic voltammetric method was developed for the sensitive and selective determination of Co<sup>II</sup> at a 1-(2-pyridylazo)-2-naphthol modified carbon paste electrode. The analysis procedure consisted of an open circuit accumulation step in stirred sample solution. This was followed by medium exchange to a 'clean' solution where the accumulated Co<sup>II</sup> was oxidized and subsequently a cathodic potential scan was effected to obtain the voltammetric peak. The precisions obtained for 10 successive determinations each of  $1.00 \times 10^{-6}$  mol l<sup>-1</sup>,  $1.00 \times 10^{-7}$  mol l<sup>-1</sup> and  $1.00 \times 10^{-8}$  mol l<sup>-1</sup> Co<sup>II</sup> were 2.80, 5.14 and 9.67% (relative standard deviations), respectively. The detection limit was estimated to be  $5.9 \times 10^{-9}$  (0.35 ppb) (S/N = 3), for 180 s accumulation. Of the 35 selected substances examined for interferences, only V<sup>II</sup>, Ce<sup>III</sup>, EDTA and Triton X-100 interfered. These interferences could be easily eliminated. The developed method was tested using a certified sample (USEPA WP 386) and then applied to the determination of Co<sup>II</sup> in human hair, pig liver and spinach samples.**

**Keywords:** Modified carbon paste electrode; cobalt(II); differential pulse cathodic voltammetry; biological materials

Although cobalt is a rare element, it is widely distributed in nature, with abundance in the Earth's crust of about 0.0001–0.0002%. The most common oxidation state is +2 and +3 with the cobaltous salts being generally stable in air but not the cobaltic.<sup>1</sup> Cobalt is present only at low levels in drinking water (0.1–5 µg l<sup>-1</sup>) and in ambient air (0.3–2.3 ng m<sup>-3</sup>).<sup>2</sup> The estimated daily intake of cobalt by humans is about 5–45 µg. The levels of Co found in human body fluids are generally low, being about 0.33 µg l<sup>-1</sup> in serum or plasma, 0.5–3.9 µg l<sup>-1</sup> in blood and 0.4 µg l<sup>-1</sup> in urine.<sup>1</sup> Cobalt is an essential element for both plants and animals. In plants, it is required for nitrogen assimilation while it is a metallic component of vitamin B<sub>12</sub> in animals. Although Co is not highly toxic, acute and chronic poisoning give rise to symptoms such as pulmonary edema, nausea, allergy and other disorders.<sup>1,3</sup>

From the above, it is obvious that to monitor Co in the natural environment, in biological systems and in various other real samples, detection at trace and ultratrace levels is necessary. Methods which have been used to determine cobalt include atomic absorption spectrometry (AAS),<sup>4,5</sup> neutron activation analysis (NAA),<sup>6</sup> X-ray fluorescence,<sup>7</sup> inductively coupled plasma mass spectrometry (ICP-MS),<sup>8</sup> inductively coupled plasma atomic emission spectrometry (ICP-AES),<sup>9</sup> etc. Of the electrochemical methods, polarography has not been widely used because of the poor reversibility at the mercury electrode, the high reduction potentials and the generally unfavorable properties of the Co–Hg amalgam.<sup>10,11</sup> However, the adsorptive stripping technique at the mercury electrode has been exploited by several investigators. The adsorption of the cobalt–dimethylglyoxime complex at mercury has been the subject of several

reports.<sup>12–15</sup> In these studies, detection limits were 0.0016–0.05 µg l<sup>-1</sup> ( $2.7 \times 10^{-11}$ – $8.5 \times 10^{-10}$  mol l<sup>-1</sup>). Zhang<sup>16</sup> formed a Co<sup>II</sup>–4-[2-(5-bromopyridylazo)-1,3-dihydroxy]naphthalene complex which, in the presence of Triton X-100, gave an adsorptive polarographic peak at –0.90 V vs. Ag/AgCl (saturated KCl). The detection limit was  $5.0 \times 10^{-10}$  mol l<sup>-1</sup>. In another study, Han *et al.*<sup>17</sup> employed differential pulse adsorptive stripping of Co<sup>II</sup>–1-nitroso-2-naphthol chelate at a static mercury drop electrode to obtain a detection limit of  $8.5 \times 10^{-10}$  mol l<sup>-1</sup> with an accumulation time of 2 min. Although these determinations by adsorptive stripping have very good detection limits, the adsorptive stripping peaks usually occur at high negative potentials (in the region of –1.0 V or even more negative<sup>12–17</sup>). In real samples, operations at such highly negative potentials involve a high probability of occurrences of interferences from the reduction of coexisting background substances.

One increasingly popular approach to minimize interferences in electroanalysis is through the use of chemically modified electrodes (CMEs).<sup>18–20</sup> The incorporation of specially chosen modifiers in the electrodes for collection of the analytes prior to voltammetric analysis gives rise to high selectivity and sensitivity. Coupled with a medium exchange step, additional discrimination against background interferences can be achieved because the voltammetric process is performed in a 'clean' background. However, literature reports on the use of CMEs for Co<sup>II</sup> determination have been rather scarce. Kasem and Abruna<sup>21</sup> modified a carbon paste electrode (CPE) with 1,10-phenanthroline for Co determination and obtained a rather high detection limit of  $1 \times 10^{-6}$  mol l<sup>-1</sup> (2 min accumulation) which they attributed to impurities in the buffer used. Gao *et al.*<sup>22</sup> also used a CPE but modified with perfluorinated sulfonated polymer–2,2-bipyridyl. Using differential pulse anodic stripping voltammetry, they obtained a detection limit of  $3 \times 10^{-7}$  mol l<sup>-1</sup> for 5 min preconcentration. In this case, interferences were observed from Cu<sup>2+</sup>, Fe<sup>2+</sup>, Ru<sup>3+</sup>, Ni<sup>2+</sup>, CN<sup>-</sup> and SCN<sup>-</sup>.

In our laboratories, we are interested in developing highly sensitive and selective methods for the determination of metal ions using CMEs. In this work, we studied the feasibility of using a 1-(2-pyridylazo)-2-naphthol (PAN) modified carbon paste electrode (PAN-MCPE) for the differential pulse cathodic determination of Co<sup>II</sup>. PAN was chosen as the modifier because it has high stability and low solubility in water, attributes desirable for modifier function. Further, it is known to complex Co<sup>II</sup> strongly<sup>23–25</sup> and has been used as a complexing agent in the spectrophotometric determination of Co<sup>II</sup>.<sup>25</sup> To further minimize interferences, a medium exchange step was incorporated. Factors affecting the accumulation and voltammetric peak of cobalt were examined. An optimized procedure was established and tested for Co<sup>II</sup> determination in a United States Environmental Protection Agency water pollution control sample (USEPA WP 386). Finally, the method was applied to the determination of Co<sup>II</sup> in human hair, pig liver and spinach.

## Experimental

### Reagents

All reagents were of analytical-reagent grade unless otherwise specified. Containers (glassware, polyethylene bottles, etc.) were soaked overnight in 10% nitric acid. Water was obtained from a Millipore Alpha-Q water purification system (Millipore Corporation, Bedford, MA, USA).

A stock solution of  $\text{Co}^{\text{II}}$  ( $1.00 \times 10^{-2} \text{ mol l}^{-1}$ ) was prepared by dissolving cobalt(II) sulfate (Merck, Darmstadt, Germany) in  $0.10 \text{ mol l}^{-1}$  nitric acid. This was stored in a darkened glass bottle. Test solutions were diluted from this stock. Britton–Robinson buffer was obtained by first preparing a mixture of phosphoric, acetic and boric acids, each  $0.040 \text{ mol l}^{-1}$ . This B–R acid mixture was then titrated to the required pH with sodium hydroxide. All other solutions were prepared using standard laboratory procedures.

Graphite powder (Merck), liquid paraffin (boiling range at 1000 hPa: 300–400 °C, dynamic viscosity (20 °C): 25–80 mPa s, (Merck) and PAN (Merck, Poole, Dorset, UK) were used as received for fabrication of CPE and PAN–MCPE.

### Apparatus

All electrochemical experiments were performed with a Princeton Applied Research Corporation Model 264A polarographic analyzer–stripping voltammeter (EG&G, Princeton, NJ, USA). Voltammograms were recorded with a Graphtec Model WX-2400 (Graphtec Corporation, Tokyo, Japan)  $x$ – $y$  recorder. A locally fabricated three electrode glass cell of about 5 ml capacity was used. The reference electrode (Ag/AgCl, saturated KCl) was placed in a compartment separated from the working electrode compartment by a salt bridge. The counter electrode was a Pt disk (3 mm diameter). pH measurements were made with a Hanna Instruments (Woonsocket, RI, USA) Model HI 9318 meter. Microwave digestions were carried out in a CEM Corporation Model MDS-2000 Series microwave sample preparation system (CEM Corporation, Matthews, USA). All experiments were performed at an ambient temperature of  $25 \pm 1$  °C.

### Fabrication of CPE and PAN–MCPE

PAN–paraffin oil–carbon powder paste (0.010% to 5.0% mass of PAN to mass of paste) was prepared by first thoroughly mixing the desired amounts of PAN and carbon powder in a mortar. Subsequently, paraffin oil was added and mixing was continued until a homogeneous paste was obtained. The unmodified CPE was prepared in the same manner but without the addition of any PAN.

For electrode fabrication, the prepared paste was packed into one end of a glass tube (approximately 2.2 mm bore) and a 2 mm diameter copper wire with a pointed tip was inserted into the other end to make electrical contact. A fresh electrode surface can be rapidly generated by extruding a small plug of the paste by pushing with the copper rod, scraping off the excess and smoothing on a piece of stiff, white paper until a shiny, smooth surface is obtained.

### Procedure

A fresh surface was generated before the commencement of each experiment. Each determination consisted of a three step operation as indicated below.

#### Accumulation step

Cobalt(II) was accumulated, at open circuit, by dipping the electrode in 25.00 ml of a stirred  $0.075 \text{ mol l}^{-1} \text{ NH}_3$  solution

containing  $\text{Co}^{\text{II}}$  in a 50 ml beaker for an accumulation time,  $t_a$  (typically 120 s or 180 s). Stirring was done with a Teflon coated magnetic stirring bar. After the accumulation period, the electrode was removed, rinsed with water and dried with absorbent paper.

#### Oxidation step

The electrode was then placed in the electrochemical cell containing deaerated (sparging with purified nitrogen for about 8 min)  $0.10 \text{ mol l}^{-1}$  potassium hydroxide solution. The accumulated  $\text{Co}^{\text{II}}$  at the electrode surface was then oxidized at a potential,  $E_o$  (+0.40 V) for a time interval  $t_o$  (30 s), without stirring.

#### Differential pulse (cathodic) voltammetric step

After the oxidation step, the potential was scanned in the negative direction from an initial value  $E_i$  ( $= E_o = +0.40 \text{ V}$ ) in the differential pulse mode (pulse amplitude 50 mV) at a scan rate of  $10 \text{ mV s}^{-1}$ , to a final potential  $E_f$  (–0.10 V). To avoid contamination, the voltammetric medium was changed after each experiment.

### Preparation of samples for cobalt determination

The USEPA WP 386 used for method testing contained the following constituents: Al(500), As(100), Be(100), Cd(25), Co(100), Cr(100), Cu(100), Fe(100), Hg(5.0), Mn(100), Ni(100), Pb(100), Se(25), V(250) and Zn(100), where the numbers in brackets are the concentrations in  $\mu\text{g l}^{-1}$ . This sample was prepared simply by pipetting 0.25 ml into a calibrated flask and making to mark with  $0.075 \text{ mol l}^{-1} \text{ NH}_3$ .

The hair, liver and spinach samples were first dried in the oven at 102 °C to constant weight before digestion using closed vessel microwave sample preparation techniques.<sup>26,27</sup> In each case, about 0.5 g of sample was used. The heating parameters for the microwave digestion are shown in Table 1. After digestion, the pH of the sample was brought up to 10.22 with concentrated ammonia solution. The sample was then transferred to a 50 ml calibrated flask and made to mark with  $0.075 \text{ mol l}^{-1} \text{ NH}_3$ . The cobalt concentration was then determined by the optimized method. Spiked experiments were also performed.

## Results and discussion

### Cyclic voltammetric studies

At the CPE in  $0.10 \text{ mol l}^{-1} \text{ KOH}$ , anodic and cathodic background breakdown occurred at about +0.85 V and –1.50 V, respectively. There was an elongated reduction wave starting at about –0.30 V. This wave was not removed even with prolonged and vigorous sparging with purified nitrogen and was attributed to the reduction of oxygen absorbed in the paste or

**Table 1** Microwave digestion parameters

Sample	Step	Power (% of 630 W)	Time/min	Pressure/ psi
Hair*	1	50	10	60
	2	30	10	100
	3	10	20	120
Spinach†	1	100	30	120
Pig liver‡	1	100	30	120

\* 0.5021 g of hair (dry mass) + 10 ml concentrated  $\text{HN}_3$  + 2 ml  $\text{H}_2\text{O}_2$ . Temperature control: off. † 0.5032 g of spinach (dry mass) + 5 ml concentrated  $\text{HNO}_3$  + 2 ml  $\text{H}_2\text{O}$ . Temperature control: off. ‡ 0.5063 g liver (dry mass) + 5 ml concentrated  $\text{HNO}_3$  + 2 ml  $\text{H}_2\text{O}$ .

adsorbed on the carbon particles.<sup>28</sup> At the PAN-MCPE, also in 0.10 mol l<sup>-1</sup> KOH, the cyclic voltammogram (CV) revealed that PAN was reduced irreversibly starting at about -0.70 V, with the reduction wave peaking at -0.85 V. PAN was also irreversibly oxidized with a broad wave commencing at +0.30 V and peak potential at +0.50 V (CVs for the above experiments are not shown here).

Fig. 1(a) shows the CV at the CPE in 0.10 mol l<sup>-1</sup> KOH after preconcentration in the blank accumulation medium. In the potential range studied, only residual current was observed. For the same experiment using PAN-MCPE, a similar result was obtained [Fig. 1(b)] except that there was an anodic current at the initial region arising from the oxidation of PAN. When the experiment was performed with 1.00 × 10<sup>-5</sup> mol l<sup>-1</sup> Co<sup>II</sup> in the accumulation medium, the same featureless CV was obtained using the CPE [Fig. 1(c)]. However, when the PAN-MCPE was employed for the open circuit accumulation, the presence of a surface cathodic peak (*E*<sub>p</sub> = +0.15 V) was obvious [Fig. 1(d)]. Corresponding to this, there was an anodic peak with peak potential at +0.19 V on the reverse scan [Fig. 1(d)]. Although there was a separation of about 40 mV between the surface redox peaks, it seemed that there was some degree of reversibility of the redox processes. However, we did not study this in greater detail. Also, we have not come across any previous studies of the electrochemical behaviors of Co-PAN complexes in the literature to make any comparison with the results observed here. It is clear from these experiments that the presence of PAN in the CPE enabled the preconcentration of Co<sup>II</sup> at the electrode surface through the formation of the Co<sup>II</sup>-PAN complex. It would appear from Fig. 1(d) that, analytically, both the cathodic and anodic surface processes could be exploited. However, as can be seen from this figure, the anodic peak is close to the foot of the oxidation wave of PAN. Due to this, our experiments indicated that although the anodic peak was potentially more sensitive than the cathodic peak, its repeatability and detection limit were poorer due to interference from PAN oxidation, especially at low concentrations of the analyte. The decision was therefore made to employ cathodic voltammetry for subsequent work.

Fig. 2 shows a representative differential pulse cathodic voltammogram at the PAN-MCPE. The peak height was found to increase with increasing concentration of Co<sup>II</sup> and also with increasing accumulation time.

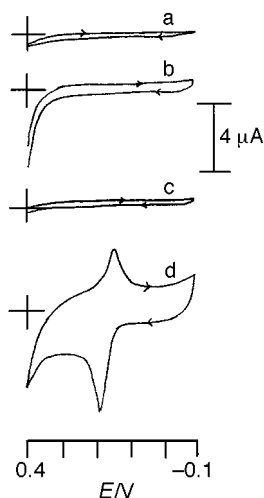
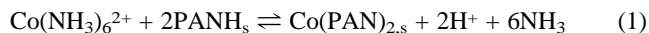


**Fig. 1** Cyclic voltammograms in 0.10 mol l<sup>-1</sup> KOH. Open circuit accumulation in 0.075 mol l<sup>-1</sup> NH<sub>3</sub>; *t*<sub>a</sub> = 120 s: (a) CPE, no Co<sup>II</sup> in accumulation medium; (b) PAN-MCPE (1.0%), no Co<sup>II</sup> in accumulation medium; (c) CPE, 1.00 × 10<sup>-5</sup> mol l<sup>-1</sup> Co<sup>II</sup> in accumulation medium; and (d) PAN-MCPE (1.0%), 1.00 × 10<sup>-5</sup> mol l<sup>-1</sup> Co<sup>II</sup> in accumulation medium. All at a scan rate of 50 mV s<sup>-1</sup>.

From the above observations, under the conditions of the experiments, the possible pathways for the analysis cycle, from accumulation to voltammetric scan, are postulated below:

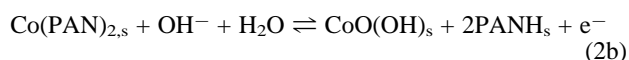
#### Accumulation



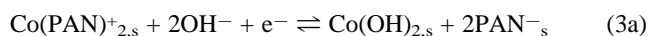
#### Oxidation



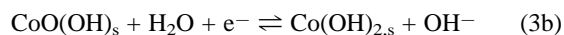
or



#### Differential pulse (cathodic) voltammetric scan



or



where subscript 's' denotes the electrode surface.

PAN is a terdentate ligand which usually forms complexes of the form M(PAN)X (X is a unidentate ligand) or M(PAN)<sub>2</sub> with metal ions, M.<sup>23</sup> In the case of Co<sup>II</sup> and Co<sup>III</sup>, various workers<sup>23,25,29</sup> have proposed the second type of complexes. During the oxidation step, two possibilities exist, the first of which is the oxidation of the surface bound complex in which the cobalt achieved an oxidation state of +3 [eqn. (2a)]. The complexation of PAN with Co<sup>III</sup> has been reported to be even stronger compared to Co<sup>II</sup>.<sup>25,30</sup> Alternatively, in the presence of hydroxyl ions (the medium was KOH), the oxidation product could be CoO(OH), as shown by eqn. (2b).<sup>31</sup> Unfortunately, we have no additional data to conclude either way at this point. However, depending on the oxidation step, the differential pulse cathodic potential scan step could again take two courses. If eqn. (2a) were the predominant reaction in the oxidation step, then the cathodic process would be according to eqn. (3a). On the other hand, eqn. (2b) led to eqn. (3b). For the cathodic step, additional data were available from the variation of the differential pulse voltammetric peak potential with KOH concentration. It was found that as the KOH concentration increased from 0.010 mol l<sup>-1</sup> to 1.00 mol l<sup>-1</sup>, the peak potential decreased from +0.28 V to +0.025 V (Table 2). Thus, increasing OH<sup>-</sup> concentration made reduction more difficult. This is consistent with eqn. (3b) rather than (3a). Based on this evidence, the processes occurring during the oxidation and stripping steps are proposed to be those of eqns. (2b) and (3b),

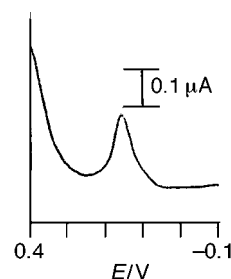


**Fig. 2** Differential pulse cathodic voltammogram at the PAN-MCPE: 1% m/m PAN; accumulation, 0.075 mol l<sup>-1</sup> NH<sub>3</sub> containing 2.50 × 10<sup>-7</sup> mol l<sup>-1</sup> Co<sup>II</sup>; differential pulse voltammetry, 0.10 mol l<sup>-1</sup> KOH; *t*<sub>a</sub> = 120 s, *t*<sub>o</sub> = 30 s, *E*<sub>o</sub> = *E*<sub>i</sub> = +0.40 V; scan rate = 10 mV s<sup>-1</sup>.

respectively. The data of Table 2 clearly establish the dependence of the voltammetric reduction process on  $\text{OH}^-$  concentration. However, a quantitative relationship is more uncertain. For example, the relationship between equilibrium redox (or formal) potentials and  $\log(\text{concentration of KOH}, C_{\text{KOH}})$  can be used to support the proposed voltammetric reduction process. But the reversibility of this process was not studied. Fig. 1(d) shows that there is a separation of about 40 mV between the oxidation and reduction peaks and this separation may be medium and composition dependent. Another problem is that for the data of Table 2, no attempt was made to control the ionic strength to a constant value. Nevertheless, a plot of the data of Table 2 [*i.e.*, peak potentials *versus*  $\log(C_{\text{KOH}})$ ], not shown here) revealed an approximate linear relationship. A linear regression analysis of this data gave the equation

$$E_p (\text{V}) = 0.029 - 0.1241 \log C_{\text{KOH}} (\text{mol l}^{-1})$$

with a correlation coefficient of  $-0.998$ . The above equation contradicts the process as given by eqn. (3b) because a slope of 59 mV ( $25^\circ\text{C}$ ) is expected instead of 124 mV shown above. At this point, we have no explanation for the discrepancy. However, we do think that the foundation for such a quantitative relationship is weak in the present case and a more detailed study is necessary.

### Factors affecting the differential pulse cathodic peak current

#### Effect of PAN loading

The effect of PAN loading from 0.10% to 5.0% m/m was studied. Initially, at lower PAN loadings, the voltammetric peak current increased with increasing PAN loadings, up to 1.0%, after which the peak current remained essentially constant until 2.0%. On further increases in PAN loadings, the peak current dropped. The decrease at PAN loadings above 2.0% was attributed to the reduced effectiveness of the CPE at high modifier contents, possibly coupled with increase in resistance.<sup>32</sup> A 1.0% PAN loading was selected for further studies.

#### Effect of accumulation medium

Various media were examined for  $\text{Co}^{\text{II}}$  accumulation. Acidic media tested were acetate buffer (pH 3.39, 4.93 and 5.00), citrate buffer (pH 3.09, 4.98) and B-R buffer (pH 5.50). Other neutral-alkaline media investigated were  $0.10 \text{ mol l}^{-1}$  ammonium chloride,  $0.10 \text{ mol l}^{-1}$  ammonium acetate,  $0.10 \text{ mol l}^{-1}$  KOH,  $0.10 \text{ mol l}^{-1}$  sodium borate (pH 9.13),  $0.10 \text{ mol l}^{-1}$   $\text{NH}_3$  (pH 10.35),  $0.10 \text{ mol l}^{-1}$  sodium carbonate (pH 11.01), borate buffer (pH 10.09), B-R buffer (pH 9.37, 10.36),  $\text{NaHCO}_3$ -NaOH (pH 10.06), phosphate-borax buffer (pH 9.00), ammonia-ammonium chloride buffer (pH 9.77, 10.51) and ammonia-ammonium carbonate buffer (pH 8.64, 9.72).

No voltammetric peaks were observed when acidic or neutral media were used to accumulate  $\text{Co}^{\text{II}}$ . This can be understood from eqn. (1). Further, the  $\text{p}K_a$  for the phenolic proton of PAN is 11.6.<sup>23</sup> Therefore, we can expect that the most favorable conditions for complexation were those at higher pH. Of the basic media, only  $0.10 \text{ mol l}^{-1}$   $\text{NH}_3$ ,  $0.10 \text{ mol l}^{-1}$  sodium

carbonate and sodium borate-NaOH buffer (pH 10.09) gave rise to a differential pulse voltammetric peak. The best sensitivity and peak shape were manifested with  $0.10 \text{ mol l}^{-1}$   $\text{NH}_3$  and this was chosen for further studies. The others were not conducive for  $\text{Co}^{\text{II}}$  accumulation probably because of hydroxide formation due to excessively high pH and/or competitive complexation of  $\text{Co}^{\text{II}}$  by components of the media. Another factor leading to poor accumulation of  $\text{Co}^{\text{II}}$  was the higher solubility of PAN with increasing pH.<sup>23</sup> The influence of pH was further demonstrated by varying the ammonia concentration of the accumulation medium. Fig. 3 shows that there is a narrow region of concentration, from  $0.0625$  to  $0.0875 \text{ mol l}^{-1}$   $\text{NH}_3$  (pH 10.10–10.25) which was optimal for  $\text{Co}^{\text{II}}$  accumulation. The voltammetric peak height decreased on both sides of this region probably for the same reasons discussed above. Thus, the final choice of accumulation medium was  $0.075 \text{ mol l}^{-1}$   $\text{NH}_3$  (pH 10.19).

#### Effect of the differential pulse voltammetric medium

The media investigated for differential pulse voltammetry were  $\text{HNO}_3$ ,  $\text{HCl}$ ,  $\text{H}_2\text{SO}_4$ ,  $\text{HClO}_4$ ,  $\text{KCl}$ ,  $\text{NaClO}_4$ ,  $\text{KNO}_3$ ,  $\text{K}_2\text{SO}_4$ ,  $\text{KOH}$ ,  $\text{NH}_3$ ,  $\text{Na}_2\text{CO}_3$ ,  $\text{Na}_3\text{PO}_4$  and  $\text{Na}_2\text{B}_4\text{O}_7$ , all at  $0.10 \text{ mol l}^{-1}$ . The alkaline media were far superior compared to the acidic and neutral media in terms of sensitivity and peak symmetry. This was because acidic conditions were not favorable for the oxidation step, as shown by eqn. (2b). At the oxidation potential of  $+0.40 \text{ V}$  employed for the oxidation step, the oxidation of the complex may not occur or may occur at a slow rate under these circumstances. Amongst the basic media,  $0.10 \text{ mol l}^{-1}$  KOH gave the most sensitive voltammetric peak. Fig. 4 shows the variation of the voltammetric peak height as a function of KOH

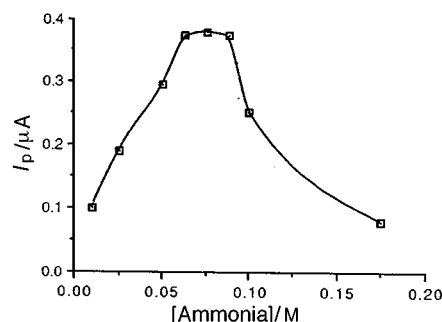


Fig. 3 Plot of differential pulse voltammetric peak current *versus* concentration of  $\text{NH}_3$  in accumulation medium: 1% m/m PAN; accumulation, ammonia solution containing  $1.00 \times 10^{-6} \text{ mol l}^{-1}$   $\text{Co}^{\text{II}}$ ; differential pulse voltammetry,  $0.10 \text{ mol l}^{-1}$  KOH;  $t_a = 120 \text{ s}$ ,  $t_o = 30 \text{ s}$ ,  $E_o = E_i = +0.40 \text{ V}$ ; scan rate =  $10 \text{ mV s}^{-1}$ .

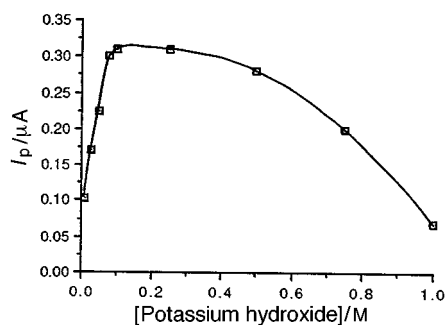


Fig. 4 Plot of differential pulse voltammetric peak current *versus* concentration of KOH in voltammetric medium: 1% m/m PAN; accumulation,  $0.075 \text{ mol l}^{-1}$   $\text{NH}_3$  containing  $1.00 \times 10^{-6} \text{ mol l}^{-1}$   $\text{Co}^{\text{II}}$ ; differential pulse voltammetry, KOH solution. All other parameters same as for Fig. 3.

Table 2 Peak potentials for differential pulse cathodic voltammograms at different KOH concentrations

KOH/ mol l <sup>-1</sup>	0.01	0.025	0.050	0.075	0.10	0.25	0.50	0.75	1.00
E <sub>p</sub> /V	0.28	0.23	0.19	0.16	0.15	0.11	0.075	0.040	0.025

concentration. As can be seen, the peak height reached a maximum value at  $0.10 \text{ mol l}^{-1}$  KOH. In KOH solutions, the redox potential of the  $\text{Co}^{\text{II}}/\text{Co}^{\text{III}}$  couple shifted towards more positive values with decreasing  $\text{OH}^-$  concentration, as discussed earlier (Table 2). This could explain the decrease in peak height at the low concentration end of Fig. 4 since the applied oxidation potential of  $+0.40 \text{ V}$  may not be sufficient for complete oxidation of the accumulated  $\text{Co}^{\text{II}}$ . On the other hand, the more gradual decrease of the peak height with increasing  $\text{OH}^-$  concentration may be due to the increased solubility of PAN at higher pH,<sup>23</sup> causing deterioration of the electrode surface.

#### Effect of oxidation potential, $E_o$ and oxidation time, $t_o$

Fig. 5 shows that, for the conditions employed here, the differential pulse cathodic peak current increased with increasing  $E_o$  and reached a maximum at about  $+0.40 \text{ V}$ . Further increase in  $E_o$  led to reduced peak currents, presumably due to the detrimental effect of the irreversible oxidation of PAN noted earlier. An  $E_o$  of  $+0.40 \text{ V}$  was therefore the potential of choice. At this potential, the voltammetric peak current increased with increasing oxidation time,  $t_o$  until a  $t_o$  of  $25 \text{ s}$ , after which no further increase in peak height was observed. A  $t_o$  of  $30 \text{ s}$  was judged to be sufficient and was adopted.

#### Effect of accumulation time, $t_a$

The variation of the voltammetric peak current with accumulation time,  $t_a$  was next investigated for three different concentrations of  $\text{Co}^{\text{II}}$ , namely,  $5.00 \times 10^{-6}$ ,  $5.00 \times 10^{-7}$  and  $5.00 \times 10^{-8} \text{ mol l}^{-1}$ . The results are shown in Fig. 6. It is obvious from this figure that the rate of accumulation of  $\text{Co}^{\text{II}}$  was the fastest at the highest concentration, as evidenced by the slope of the rising portions of the plots. Further, equilibrium was attained after about  $90 \text{ s}$ ,  $180 \text{ s}$  and  $300 \text{ s}$  for the  $\text{Co}^{\text{II}}$  concentrations of  $5.00 \times 10^{-6}$ ,  $5.00 \times 10^{-7}$  and  $5.00 \times 10^{-8} \text{ mol l}^{-1}$ , respectively. As can be expected, for a given  $t_a$ , the stripping peak current was higher for a more concentrated solution.

#### Calibration, precision and detection limit

The differential pulse cathodic peak currents were measured, using the set of optimum conditions, for a series of  $\text{Co}^{\text{II}}$  concentrations ranging from  $1.00 \times 10^{-8}$  to  $2.00 \times 10^{-5} \text{ mol l}^{-1}$ , for an accumulation time of  $180 \text{ s}$ . Two portions of good linearity were observed in the concentration ranges from  $1.00 \times 10^{-8}$  to  $2.50 \times 10^{-7} \text{ mol l}^{-1}$  and  $7.50 \times 10^{-7}$  to  $1.00 \times 10^{-5} \text{ mol l}^{-1}$ . For the region of lower  $\text{Co}^{\text{II}}$  concentrations, linear regression analysis gave

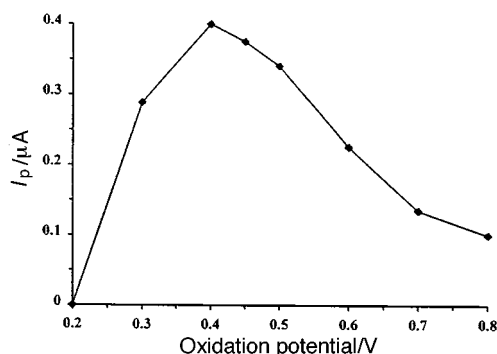


**Fig. 5** Plot of differential pulse voltammetric peak current versus oxidation potential,  $E_o$ ;  $E_i = +0.40 \text{ V}$  for  $E_o$  greater than or equal to  $+0.40 \text{ V}$ ; otherwise  $E_i = E_o$ ; accumulation,  $0.075 \text{ mol l}^{-1} \text{ NH}_3$  containing  $1.00 \times 10^{-6} \text{ mol l}^{-1} \text{ Co}^{\text{II}}$ ; differential pulse voltammetry,  $0.10 \text{ mol l}^{-1} \text{ KOH}$ . All other parameters same as for Fig. 3.

$$i_p (\mu\text{A}) = 0.0097 + 0.759C (\mu\text{mol l}^{-1})$$

with a correlation coefficient of  $0.9987$  (6 points). In the higher concentration region, the linear regression equation is

$$i_p (\mu\text{A}) = 0.0488 + 0.365C (\mu\text{mol l}^{-1})$$

with correlation coefficient  $0.9999$  (6 points). The existence of two different linear regions in the calibration plot was due to the different factors controlling  $\text{Co}^{\text{II}}$  accumulation. For the lower concentration range, the equilibrium region has not been reached at  $t_a$  of  $180 \text{ s}$  (see Fig. 6) so that accumulation was largely controlled by the rate of  $\text{Co}^{\text{II}}$  uptake. However, for the higher concentration linear range, equilibrium has been attained at the same  $t_a$  (Fig. 6). In the concentration range  $2.50 \times 10^{-7}$  to  $7.50 \times 10^{-7} \text{ mol l}^{-1} \text{ Co}^{\text{II}}$ , the calibration plot was nonlinear. This was a transition region from kinetic to equilibrium control where mixed control of  $\text{Co}^{\text{II}}$  uptake gave rise to curvature. Beyond  $1.00 \times 10^{-5} \text{ mol l}^{-1} \text{ Co}^{\text{II}}$ , the calibration plot began to level off, indicating the onset of complexing sites saturation. The detection limit was estimated to be  $5.9 \times 10^{-9} \text{ mol l}^{-1} \text{ Co}^{\text{II}}$  ( $0.35 \text{ ppb}$ ) ( $S/N = 3$ ), for  $180 \text{ s}$  accumulation. This could possibly be improved for a longer accumulation time. The precisions obtained for 10 successive determinations each of  $1.00 \times 10^{-6}$ ,  $1.00 \times 10^{-7}$  and  $1.00 \times 10^{-8} \text{ mol l}^{-1} \text{ Co}^{\text{II}}$  were  $2.80$ ,  $5.14$  and  $9.67\%$  (relative standard deviations), respectively. These good precisions obtained reflect the ability of the chemically modified CPE to provide a rapidly renewable and reproducible surface under controlled conditions. This is an advantageous feature of CMCPs in electroanalysis. In the context of metal ions analysis, it is frequently true that, due to the high affinity of the modifier for the metal ion under study as occurred here, the removal of the accumulated metal ion from the electrode surface is difficult. In such cases, generating a new and reproducible surface is the method of choice. Of course, if the accumulated analyte could be readily removed without any deleterious effect on the electrode surface, the re-use of the same surface is also possible.

#### Effect of other ions, complexing agents and surfactant

The presence of other metal ions could interfere with  $\text{Co}^{\text{II}}$  determination if they compete for complexation at the PAN complexing sites. When the developed procedure was employed for the determination of  $1.00 \times 10^{-6} \text{ mol l}^{-1} \text{ Co}^{\text{II}}$  with an accumulation time of  $120 \text{ s}$ , no interference was encountered for additions of  $2.00 \times 10^{-5} \text{ mol l}^{-1}$  each of  $\text{Na}^+$ ,  $\text{Ag}^+$ ,  $\text{Be}^{\text{II}}$ ,  $\text{Ni}^{\text{II}}$ ,  $\text{Zn}^{\text{II}}$ ,  $\text{Cd}^{\text{II}}$ ,  $\text{Cu}^{\text{II}}$ ,  $\text{Pb}^{\text{II}}$ ,  $\text{Ca}^{\text{II}}$ ,  $\text{Mn}^{\text{II}}$ ,  $\text{Ba}^{\text{II}}$ ,  $\text{Mg}^{\text{II}}$ ,  $\text{Sn}^{\text{II}}$ ,  $\text{Ge}^{\text{II}}$ ,  $\text{Al}^{\text{III}}$ ,  $\text{Cr}^{\text{III}}$ ,  $\text{Fe}^{\text{III}}$ ,  $\text{As}^{\text{III}}$ ,  $\text{Bi}^{\text{III}}$ ,  $\text{Sb}^{\text{III}}$ ,  $\text{In}^{\text{III}}$ . Vanadium(II) and  $\text{Ce}^{\text{III}}$  at  $1.00 \times 10^{-5}$

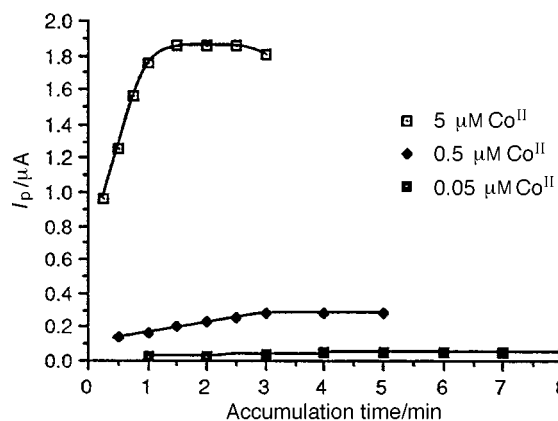


**Fig. 6** Plot of differential pulse voltammetric peak current versus accumulation time,  $t_a$ ; accumulation,  $0.075 \text{ mol l}^{-1} \text{ NH}_3$  containing:  $5.00 \times 10^{-8} \text{ mol l}^{-1} \text{ Co}^{\text{II}}$  (■);  $5.00 \times 10^{-7} \text{ mol l}^{-1} \text{ Co}^{\text{II}}$  (◆);  $5.00 \times 10^{-6} \text{ mol l}^{-1} \text{ Co}^{\text{II}}$  (□). Differential pulse voltammetry,  $0.10 \text{ mol l}^{-1} \text{ KOH}$ . All other parameters same as for Fig. 3.

mol l<sup>-1</sup> also did not interfere. However, the presence of  $2.00 \times 10^{-5}$  mol l<sup>-1</sup> V<sup>II</sup> and Ce<sup>III</sup> caused 33% and 42% depressions of the Co<sup>II</sup> peak, respectively. Interferences from both these ions could be eliminated by masking with  $1.00 \times 10^{-3}$  mol l<sup>-1</sup> sodium citrate.

Organic and other inorganic materials can also interfere either by competitive complexation of Co<sup>II</sup> in solution or other processes. In the determination of  $1.00 \times 10^{-6}$  mol l<sup>-1</sup> Co<sup>II</sup>, no interference was found after addition of  $1.00 \times 10^{-3}$  mol l<sup>-1</sup> each of KBr, KCl, KSCN, sodium citrate, sodium diethyldithiocarbamate, ammonium tartrate, (NH<sub>2</sub>)<sub>2</sub>CO, (NH<sub>4</sub>)<sub>2</sub>C<sub>2</sub>O<sub>4</sub>, NH<sub>2</sub>OH.HCl and 1,10-phenanthroline. However, introduction of  $1.00 \times 10^{-3}$  mol l<sup>-1</sup> EDTA (disodium salt) resulted in 82% decrease in the Co<sup>II</sup> peak due to preferential complexation between Co<sup>II</sup> and EDTA. Addition of  $1.00 \times 10^{-3}$  mol l<sup>-1</sup> Triton X-100 caused the complete disappearance of the voltammetric peak, probably arising from the solubilization of the Co<sup>II</sup>-PAN chelate in the presence of the surfactant.<sup>30</sup>

### Comparison with other electrochemical methods

As mentioned earlier, the most widely studied electrochemical stripping determination of Co<sup>II</sup> is based on adsorptive (cathodic) stripping at the mercury electrode. Of the eight such studies referenced here,<sup>12-17,33,34</sup> four employed the adsorption of the Co<sup>II</sup>-dimethylglyoxime complex.<sup>12-15,33</sup> Typically, adsorption of the complex was effected at -0.75 V and the cathodic stripping occurred at slightly more negative than -1 V. Detection limits ranged from about  $4 \times 10^{-11}$  mol l<sup>-1</sup> (30 s accumulation<sup>14</sup>) to  $6.8 \times 10^{-9}$  mol l<sup>-1</sup> (30-120 s accumulation<sup>33</sup>). Although this method apparently did not give serious problems with interferences, as reported by the investigators, the high cathodic stripping peak potential for the complex is a potential source of problem in terms of background interferences. In other related works, Godlewska *et al.*<sup>33</sup> used the catalytic adsorptive stripping of the Co<sup>II</sup>-diphenylglyoxime complex at the mercury electrode while Bobrowski<sup>34</sup> studied the catalytic adsorptive stripping of the Co<sup>II</sup>-dioxime-nitrite system. In the former, a detection limit of  $5.0 \times 10^{-10}$  mol l<sup>-1</sup> Co<sup>II</sup> was obtained while in the latter the detection limit was  $3 \times 10^{-10}$  mol l<sup>-1</sup>. For these methods, *E*<sub>p</sub>s values for the stripping peaks were generally about the same as those for the Co<sup>II</sup>-dimethylglyoxime complex. Han *et al.*<sup>17</sup> also investigated adsorptive, cathodic stripping of the Co<sup>II</sup>-1-nitroso-2-naphthol complex. Here, the stripping peak was found at a considerably less negative potential of -0.51 V (vs. calomel electrode, 3

mol l<sup>-1</sup> KCl) compared to the Co(II)-dimethylglyoxime complex. The detection limit in this case was reported to be  $9 \times 10^{-10}$  mol l<sup>-1</sup> for a 2 min accumulation.

Reported works in the literature on the use of CMEs for cobalt determination are scarce. Our literature search (not exhaustive) yielded two such works. In the earlier of the two studies, Kasem and Abruna<sup>21</sup> employed a 1,10-phenanthroline modified CPE for accumulation of Co<sup>II</sup> followed by anodic stripping. The detection limit, at about  $1 \times 10^{-6}$  mol l<sup>-1</sup> Co<sup>II</sup> (2 min accumulation) was rather high and this was attributed to impurities in the buffer. Only Cu<sup>+</sup> and Fe<sup>2+</sup> were studied for interferences and it was found that these two interfered significantly at ten-fold and five-fold excess, respectively. Subsequently, Gao *et al.*<sup>22</sup> utilized a CPE modified with both Nafion and 2,2-bipyridyl for the collection of Co<sup>II</sup> followed by anodic stripping. A medium exchange step was also incorporated. For a 5 min preconcentration, the detection limit was found to be  $3 \times 10^{-7}$  mol l<sup>-1</sup>. Several ions such as Cu<sup>II</sup>, Fe<sup>II</sup>, Ru<sup>III</sup>, Ni<sup>II</sup>, CN<sup>-</sup>, and SCN<sup>-</sup> interfered.

The method developed here compares favorably with the above methods. Although the detection limit of  $5.9 \times 10^{-9}$  mol l<sup>-1</sup> is at the higher end of the adsorptive stripping methods, the stripping peak potential of +0.15 V, coupled with the medium exchange step, clearly has advantages in terms of elimination of interferences. This is demonstrated by the fact that of the twenty-three metal ions, five anions and seven other compounds studied, only two metal ions (at twenty-fold excess) and two other substances, namely, EDTA and Triton X-100 interfered. When comparisons were made to the two CMCPEs discussed here, the advantages of the present electrode, in terms of detection limit and interferences, are obvious.

### Applications to real analysis

The developed method was applied to the determination of Co<sup>II</sup> in human hair, pig liver and spinach after testing with a standard sample (USEPA WP 386). For these determinations, the calibration plot method was employed. The results are summarized in Table 3. From Table 3, in the case of the USEPA WP 386 sample, good agreement was found between the certified and the experimental values. For the real samples, satisfactory recoveries were obtained although these were typically about 8% low. These slightly low recoveries could be due to sample matrix effect. If so, this could be alleviated by using the standard addition method although this was not done here.

**Table 3** Determination of Co<sup>II</sup> in USEPA WP 386 and also in hair, liver and spinach samples\*

Sample	Certified (10 <sup>-6</sup> )	Spiked (10 <sup>-8</sup> )	Experimental (10 <sup>-8</sup> )	Recovery (%)	Concentration in original sample/g kg <sup>-1</sup>
USEPA WP 386	1.70 (5.49) <sup>§</sup>	—	1.65 <sup>†</sup> (5.2) <sup>‡</sup>	—	—
Hair	—	—	3.33 (10.3)	—	—
	—	5.0	7.95 (9.8)	92.4	211
Liver	—	—	2.02 (10.9)	—	—
	—	5.0	6.63 (10.1)	92.2	127
Spinach	—	—	2.68 (10.8)	—	—
	—	5.0	7.29 (9.9%)	92.2	170

\* Concentrations are in mol l<sup>-1</sup> unless otherwise stated. <sup>†</sup> For this sample, this value is multiplied by 10<sup>-6</sup> and not 10<sup>-8</sup>. <sup>‡</sup> Figures in brackets are relative standard deviations (%); in all cases the number of observations, *n* = 4. <sup>§</sup> Relative standard deviation (%) for certified sample provided by USEPA.

This work was supported by a grant from the National University of Singapore.

## References

- 1 Thunus, L., and Lejeune, R., in *Handbook on Metals in Clinical and Analytical Chemistry*, ed. Seiler, H. G., Sigel, A., and Sigel, H., Marcel Dekker, New York, 1994, pp. 333–338.
- 2 Tsalev, D. L., and Zaprianov, Z. K., *Atomic Absorption Spectrometry in Occupational and Environmental Health Practice*, CRC Press, Boca Raton, 1984.
- 3 McKenzie, H. A., and Smythe, L. E., *Quantitative Trace Analysis of Biological Materials*, Elsevier, New York, 1988, p. 422.
- 4 Campos, R. C., and Moraes, S. S., *At. Spectrosc.*, 1993, **14**, 71.
- 5 Trojanowicz, M., and Pyrzynska, K., *Anal. Chim. Acta*, 1994, **287**, 247.
- 6 Ambulkar, M. N., Chutke, N. L., Aggarwal, A. L., and Garg, A. N., *Sci. Total. Environ.*, 1994, **141**, 93.
- 7 Yap, C. T., and Hua, Y., *Anal. Sci.*, 1994, **10**, 49.
- 8 Al-Swaidan, H. M., *Anal. Lett.*, 1994, **27**, 145.
- 9 Uchida, T., Isoyama, H., Oda, H., Wada, H., and Uenoyama, H., *Anal. Chim. Acta*, 1993, **283**, 1575.
- 10 Hovsepian, B. K., and Shain, I., *J. Electroanal. Chem.*, 1966, **12**, 397.
- 11 Vydra, F., Stulik, K., and Julakova, E., *Electrochemical Stripping Analysis*, (Tyson, J., translation ed.), Ellis Horwood, Chichester, UK, 1976, pp. 259–261.
- 12 Gilbert, M. J. M., and Powell, H. K. J., *Anal. Chim. Acta*, 1988, **207**, 103.
- 13 Bodewig, F. G., *Mikrochim. Acta*, 1989, **111**, 75.
- 14 Bobrowski, A., and Bond, A. M., *Electroanalysis*, 1992, **4**, 975.
- 15 Westenbrink, W. W., Page, J. A., and VanLoon, G. W., *Can. J. Chem.*, 1990, **68**, 209.
- 16 Zhang, Z. Q. *Mikrochim. Acta*, 1991, **1**, 88.
- 17 Han, J., Chen, H., and Gao, H., *Electroanalysis*, 1993, **5**, 619.
- 18 Murray, R. W., in *Electroanalytical Chemistry*, ed. Bard, A. J., Marcel Dekker, New York, 1984, pp. 191–368.
- 19 Arrigan, D. W. M., *Analyst*, 1994, **119**, 1953.
- 20 Kalcher, K., Kauffman, J. M., Wang, J., Svancara, I., Vytras, K., Neuhold, C., and Yang, Z., *Electroanalysis*, 1995, **7**, 5.
- 21 Kasem, K. K., and Abruna, H. D., *J. Electroanal. Chem.*, 1988, **242**, 87.
- 22 Gao, Z., Wang, G., Li, P., and Zhao, Z., *Anal. Chem.*, 1991, **63**, 953.
- 23 Ueno, K., Imamura, T., and Cheng, K. L., *Handbook of Organic Analytical Reagents*, CRC Press, Boca Raton, FL, 2nd edn., 1992, pp. 209–217.
- 24 Corsini, A., Yih, I. M. L., Fernando, Q., and Freiser, H., *Anal. Chem.*, 1962, **34**, 1090.
- 25 Ohzeki, K., Toki, C., Ishida, R., and Saitoh, T., *Analyst*, 1987, **112**, 1688.
- 26 Bettinelli, M., Baroni, U., and Pastorelli, N., *Anal. Chim. Acta*, 1989, **225**, 159.
- 27 Kojima, I., Kato, A., Iida, C., *Anal. Chim. Acta*, 1992, **264**, 101.
- 28 Adams, R. N., *Electrochemistry at Solid Electrodes*, Marcel Dekker, New York, 1969, pp. 26, 121.
- 29 Shibata, S., *Anal. Chim. Acta*, 1961, **25**, 348.
- 30 Watanabe, H., *Talanta*, 1974, **21**, 295.
- 31 Cotton, F. A., and Wilkinson, G., *Advanced Inorganic Chemistry*, Wiley, Toronto, 1988, pp. 724–738.
- 32 Prabhu, S. V., and Baldwin, R. P., *Anal. Chem.*, 1987, **59**, 1074.
- 33 Godlewska, B., Golimski, J., Hulanicki, A., and van den Berg, C. M. G., *Analyst*, 1995, **120**, 143.
- 34 Bobrowski, A., *Anal. Chem.*, 1989, **61**, 2179.

Paper 7/07375E

Received October 13, 1997

Accepted March 31, 1998